

Photocatalytic hydrodenitrogenation of aromatic cyanides on TiO₂ loaded with Pd nanoparticles

Cite this: *Catal. Sci. Technol.*, 2013, **3**, 1718

Yoshitsune Sugano,^a Keisuke Fujiwara,^a Yasuhiro Shiraishi,^{*a} Satoshi Ichikawa^b and Takayuki Hirai^a

Photocatalytic hydrodenitrogenation of aromatic cyanides has been carried out on TiO₂ loaded with Pd nanoparticles (Pd-TiO₂) in the presence of ethanol as a hydrogen source. Photoirradiation of Pd-TiO₂ at $\lambda > 300$ nm in ethanol containing aromatic cyanides successfully produces the corresponding toluene derivatives and triethylamine with almost quantitative yields. Photoexcited Pd-TiO₂ catalysts promote oxidation of ethanol and reduction of protons, producing acetaldehyde and hydrogen atoms on the surface of Pd particles (H-Pd species). Aromatic cyanides undergo hydrodenitrogenation *via* consecutive reactions involving hydrogenation by the H-Pd species and condensation with aldehydes. The catalytic activity strongly depends on the amount of Pd loaded. The catalyst containing 2 wt% Pd, with a relatively low Schottky barrier height at the Pd-TiO₂ heterojunction and a large number of surface Pd atoms, exhibits the highest denitrogenation activity.

Received 5th November 2012,
Accepted 28th January 2013

DOI: 10.1039/c3cy20748j

www.rsc.org/catalysis

1. Introduction

Aromatic cyanides are some of the most important chemicals used as solvents, extractants, and intermediates for the synthesis of pharmaceuticals, plastics, rubbers, herbicides, and pesticides.¹ These compounds are therefore often contained in industrial effluents. Since they are highly toxic to living organisms,² their decomposition and detoxification are very important tasks. Bioremediation processes have been studied for the treatment of aromatic cyanides.³ These processes decompose the compounds into harmless ones such as CO₂ and H₂O; however, they require restricted operation conditions in pH and temperature. Photocatalytic decomposition of aromatic cyanides has also been studied with titanium dioxide (TiO₂).⁴ Photoexcitation of TiO₂ in water under O₂ produces active oxygen species such as hydroxyl radicals (OH•) or superoxide anions (O₂•⁻), and decomposes aromatic cyanides into CO₂, NO₃⁻, and H₂O.⁵ These oxidative processes, however, completely decompose the aromatic nuclei of the compounds. Selective decomposition of the -CN moiety and the reuse of resulting aromatic nuclei for upstream processes are desirable for the development of green and sustainable processes.

Supported Pd nanoparticles are often employed for catalytic hydrogenation of various compounds such as olefins⁶⁻⁹ and nitro compounds¹⁰⁻¹² with molecular hydrogen (H₂) as a hydrogen source. Hydrogenation of aromatic cyanides on Pd catalysts has also been studied at elevated temperatures.¹³ These compounds are successfully converted into toluene derivatives and NH₃ *via* hydrogenation and subsequent cleavage of the C-N moiety. This hydrodenitrogenation is promoted by the reaction of aromatic cyanides with activated hydrogen species (H-Pd), formed *via* a dissociative adsorption of H₂ on the surface of Pd particles. The reaction proceeds selectively without decomposition of aromatic nuclei and enables the reuse of products for upstream processes.

Photoexcitation of semiconductor materials loaded with noble metal particles creates a positive hole (h⁺) and conduction band electrons (e⁻), and allows subsequent e⁻ transfer to metal particles.¹⁴ Photoexcitation of semiconductors loaded with Pd particles, when performed in protic solvents such as alcohols, produces aldehydes *via* oxidation of alcohols by h⁺ and H-Pd species *via* reduction of protons (H⁺) by e⁻ on the Pd particles.¹⁵ This photocatalytic reaction, if performed with aromatic cyanides, may successfully promote hydrodenitrogenation by the photoformed H-Pd species at room temperature.

In the present work, TiO₂ loaded with Pd particles (Pd-TiO₂) was used for the photocatalytic reaction of aromatic cyanides with ethanol under UV irradiation ($\lambda > 300$ nm). This catalytic system successfully promotes hydrodenitrogenation of aromatic cyanides and produces toluene derivatives with high selectivity at room temperature. The denitrogenation mechanism was

^a Research Center for Solar Energy Chemistry, and Division of Chemical Engineering, Graduate School of Engineering Science, Osaka University, Toyonaka, 560-8531, Japan. E-mail: shiraish@cheng.es.osaka-u.ac.jp; Fax: +81-6-6850-6273; Tel: +81-6-6850-6271

^b Institute for NanoScience Design, Osaka University, Toyonaka, 560-8531, Japan

clarified, and the effect of the Pd amount on the catalytic activity was studied.

2. Experimental

2.1 Materials

All of the reagents used were purchased from Wako, Tokyo Kasei, and Sigma-Aldrich, and used without further purification. Water was purified by the Milli Q system. JRC-TIO-4 TiO₂ (equivalent to Degussa P25; particle diameter, 24 nm; BET surface area, 54 m² g⁻¹; anatase/rutile = ca. 83/17) was kindly supplied by the Catalyst Society of Japan.

The Pd_x-TiO₂ catalysts [x (wt%) = Pd/(Pd + TiO₂) × 100; x = 0.5, 1, 2, 4] were prepared according to the literature procedure¹⁶ as follows: TiO₂ (1.0 g) and Pd(NO₃)₂ (10.9, 21.9, 44.2, or 90.2 mg) were added to water (40 mL), and solvents were evaporated with vigorous stirring at 353 K for 12 h. The obtained powders were calcined at 673 K under an air flow (0.5 L min⁻¹) and then reduced at 673 K under an H₂ flow (0.2 L min⁻¹). The heating rate and the holding time at 673 K for these treatments were 2 K min⁻¹ and 2 h, respectively. Ag₂-TiO₂ and Pt₂-TiO₂ were prepared in a similar manner to Pd_x-TiO₂, using AgNO₃ (16 mg) or H₂PtCl₆·6H₂O (54 mg) as a precursor.

Au₂-TiO₂ was prepared by a deposition-precipitation method as follows:¹⁷ HAuCl₄·4H₂O (45.8 mg) was added to water (50 mL). The pH of the solution was adjusted to 7 by an addition of 1 M NaOH. TiO₂ (1.0 g) was added to the solution and stirred vigorously at 353 K for 3 h. The particles were recovered by centrifugation and washed with water. They were calcined at 673 K under an air flow (0.5 L min⁻¹).

2.2 Photoreaction procedure

Each of the respective catalysts (10 mg) was added to ethanol (5 mL) containing aromatic cyanides within a Pyrex glass tube (20 cm³; φ 16.5 mm). The tube was sealed using a rubber septum cap and purged with argon gas. Each tube was photoirradiated with magnetic stirring by an Xe lamp (2 kW; Ushio Inc.). The temperature of the solution during photoirradiation was 298 K, and the light intensity was 18.2 W m⁻² (at 300–400 nm; through a water filter). After photoirradiation, the gas phase product was analyzed by GC-TCD (Shimadzu; GC-8A). The resulting solution was recovered by centrifugation and analyzed by GC-FID (Shimadzu; GC-2010), where the products were identified by GC-MS (EI) (Shimadzu; 40 GCMS-QP5050A).

2.3 Analysis

Total amounts of metals on the catalysts were determined by an inductively-coupled argon plasma atomic emission spectrometer (ICAP-AES; SII Nanotechnology, SPS 7800), after dissolution of catalysts in aqua regia.¹⁶ Diffuse reflectance UV-vis spectra were measured on an UV-vis spectrophotometer (Jasco Corp.; V-550 with an Integrated Sphere Apparatus ISV-469) using BaSO₄ as a reference. Transmission electron microscopy (TEM) observations were carried out using an FEI Tecnai G2 20ST analytical electron microscope operated at 200 kV.

3. Results and discussion

3.1 Synthesis and characterization of catalysts

The Pd_x-TiO₂ catalysts with different Pd loadings [x (wt%) = Pd/(Pd + TiO₂) × 100; x = 0.5, 1, 2, 4] were prepared by impregnation of Pd(NO₃)₂ on to TiO₂ followed by reduction with H₂. Fig. 1 shows the typical TEM images of respective Pd_x-TiO₂ catalysts. All catalysts contain spherical Pd particles. The size of the Pd particles increases with the Pd loadings: the average diameters for x = 0.5, 1, 2, and 4 catalysts were 2.6, 4.1, 5.0, and

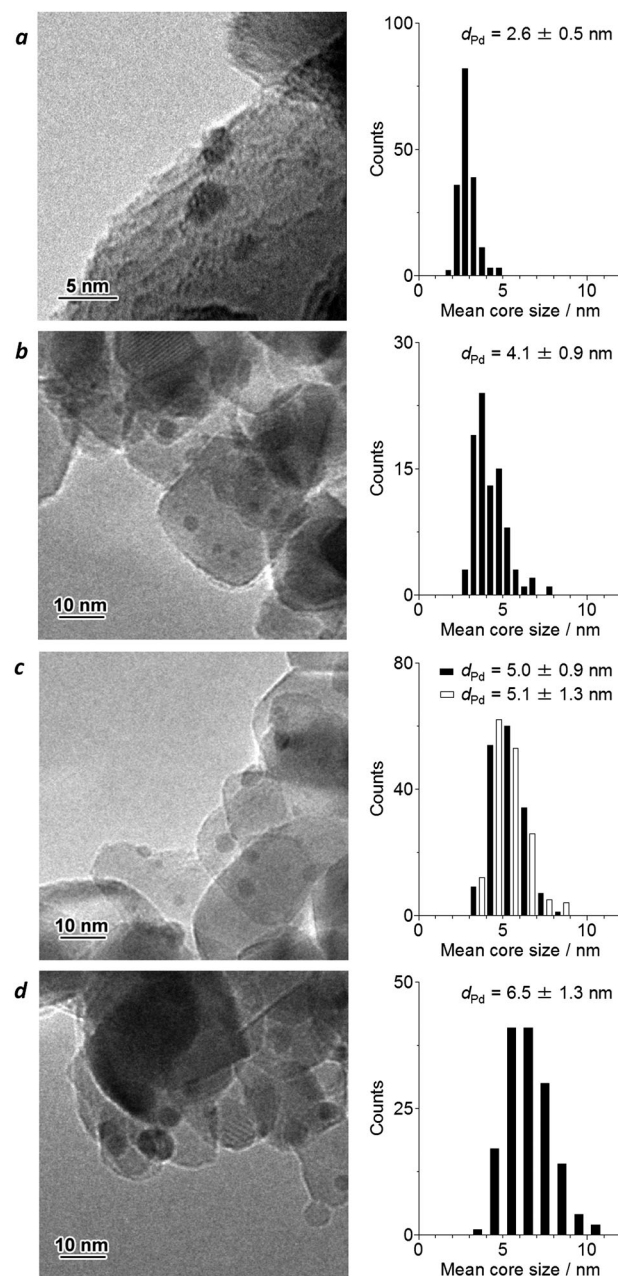


Fig. 1 TEM images and size distribution of Pd particles for (a) Pd_{0.5}-TiO₂, (b) Pd₁-TiO₂, (c) Pd₂-TiO₂, and (d) Pd₄-TiO₂ catalysts. The black bars show the data for fresh catalysts, and the white bars show the data for catalysts recovered after the 3rd reuse for reactions (Table 2, run 4).

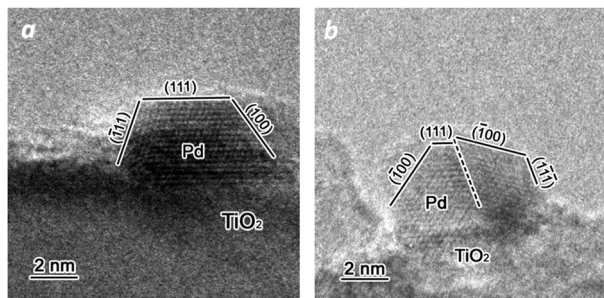


Fig. 2 High-resolution TEM images of the Pd₂-TiO₂ catalyst. (a) The incident beam direction is [0, -1, 1]. (b) This particle is a twinned particle. The incident beam directions are [0, -1, 1] and [0, 1, -1].

6.5 nm, respectively. As shown in Fig. 2, high-resolution TEM images of catalysts revealed that Pd particles can be indexed as fcc structures, as same as bulk metallic Pd (JCPDS 46-1043). Fig. 3 shows diffuse-reflectance UV-vis spectra of catalysts. The higher Pd loading catalysts exhibit increased absorbance at $\lambda > 300$ nm due to the light scattering by the Pd particles.¹⁵ As shown in the inset, TiO₂ loaded with 2 wt% Pt (Pt₂-TiO₂) exhibits spectra similar to that of Pd_x-TiO₂,¹⁸ and TiO₂ loaded with 2 wt% Au (Au₂-TiO₂) and Ag (Ag₂-TiO₂) exhibits distinctive absorption bands at 400–500 nm assigned to localized surface plasmon resonance.^{17,19}

The catalytic activity of Pd-TiO₂ for hydrodenitrogenation was studied with benzonitrile (**1**) as a model compound.¹³ Table 1 (runs 1–3) summarizes the results for the hydrodenitrogenation of benzonitrile with H₂ (1 atm) as a hydrogen source in the dark. Benzonitrile (2 mM) and Pd₂-TiO₂ (10 mg) were added to an *n*-hexane solution (5 mL) containing 5% ethanol, and the solution was stirred under H₂ (1 atm) for 6 h at different temperatures. As shown in run 1, the benzonitrile conversion at 298 K is 84% but the yield of toluene (**2**) is only 15%, where large amounts of benzylamine (**3**, 30%) and *N*-ethylbenzylamine (**4**, 38%) remain. This suggests that the C–N cleavage is difficult to achieve at this temperature. As shown in runs 2 and 3, the rise in temperature increases the

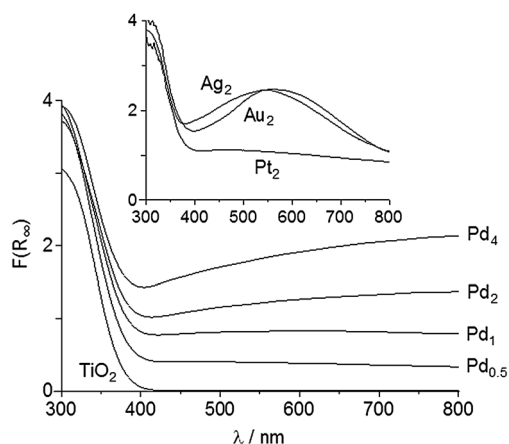


Fig. 3 Diffuse-reflectance UV-vis spectra of Pd_x-TiO₂, Pt₂-TiO₂, Au₂-TiO₂, and Ag₂-TiO₂ catalysts.

Table 1 Hydrodenitrogenation of benzonitrile with the Pd₂-TiO₂ catalyst

Run	System	Temp./K	Conversion of 1 /%	Yield/%		
				2	3	4
1 ^a	H ₂	298	84	15	30	38
2	H ₂	313	98	61	14	23
3	H ₂	333	>99	99	0	0
4 ^b	Photo	298	99	99	0	0

^a Dibenzylamine (1%) was also detected as a product. This is produced by the nucleophilic attack of a lone pair of nitrogen atoms of benzylamine to an electrophilic carbon atom of the semi-hydrogenated intermediate (ref. 13). ^b After photoreaction, acetaldehyde (197 μmol) and trace amounts of *N,N*-diethylbenzylamine (**5**) were formed.

toluene yields, and the reaction at 333 K facilitates almost quantitative conversion to toluene (run 3). The photocatalytic reaction of benzonitrile with alcohol as a hydrogen donor was carried out. The reaction was performed by photoirradiation ($\lambda > 300$ nm) of the solution under argon (1 atm) for 6 h. As shown in run 4, the reaction facilitates complete conversion of benzonitrile to toluene at 298 K. This suggests that the photocatalytic reaction with alcohol as a hydrogen source successfully promotes hydrodenitrogenation even at room temperature.

3.2 Photocatalytic activity of Pd-TiO₂ catalysts

The photocatalytic activity of Pd_x-TiO₂ with different Pd loadings (*x*) was studied in ethanol. Table 2 summarizes the results for photocatalytic reaction of benzonitrile by a 6 h reaction. As shown in run 1, pure TiO₂ promotes almost no reaction of benzonitrile. In contrast, increased Pd loadings (runs 2–5) enhance the reaction and produce toluene with high selectivity (>95%). Among the catalysts, Pd₂-TiO₂ exhibits the highest denitrogenation activity, and further Pd loading (Pd₄-TiO₂) decreases the activity. Loading of other metal particles is inefficient for denitrogenation. As shown in runs 6 and 7, Au₂-TiO₂ or Ag₂-TiO₂ promotes almost no reaction of benzonitrile. Pt₂-TiO₂ (run 8) shows a relatively high conversion of benzonitrile (45%); however, the toluene yield is only 8%, where *N,N*-diethylbenzylamine (**5**) is produced mainly (36%). These data indicate that the Pd-TiO₂ catalyst, especially loaded with 2 wt% Pd, promotes efficient denitrogenation. It must be noted that the catalyst is reusable for further reaction. As shown in run 4, the Pd₂-TiO₂ catalyst, when reused for further reaction, shows activity and selectivity similar to those of the virgin catalyst. In addition, as shown in Fig. 1c (white bars), TEM analysis of the catalyst recovered after the reaction revealed that the size of Pd particles scarcely changes during the reactions.

This indicates that the catalyst is reusable without loss of activity and selectivity.

As shown in runs 2–5 (Table 2), photoreactions with Pd-TiO₂ catalysts produced triethylamine (**6**) with the amount similar to that of toluene formed. Fig. 4 shows the time-dependent

Table 2 Photocatalytic hydrodenitrogenation of benzonitrile (1) in ethanol with various catalysts^a

Run	Catalyst	<i>d</i> /nm ^b	Conversion of 1/%	Yield/%			Acetaldehyde formed/ μ mol	H ₂ formed/ μ mol
				Toluene (2)	<i>N,N</i> -Diethylbenzylamine (5)	Triethylamine (6)		
1	TiO ₂		0	0	0	0	6	< 0.1
2	Pd _{0.5} -TiO ₂	2.6	42	40	Trace	38	293	289
3	Pd ₁ -TiO ₂	4.1	58	57	Trace	54	256	242
4	Pd ₂ -TiO ₂	5.0	>99	98	Trace	96	206	176
	1st Reuse ^c		>99	99	Trace	96		
	2nd Reuse ^c		>99	97	Trace	95		
	3rd Reuse ^c		>99	98	Trace	97		
5	Pd ₄ -TiO ₂	6.5	86	85	Trace	83	143	119
6	Au ₂ -TiO ₂	3.7	0	0	0	0	207	202
7	Ag ₂ -TiO ₂	4.6	0	0	0	0	55	51
8	Pt ₂ -TiO ₂	3.1	45	8	36	5	153	144
9	Pd ₂ -TiO ₂ ^d	5.0					263	248

^a Reaction conditions: catalyst (10 mg), benzonitrile (10 μ mol), ethanol (5 mL), Xe lamp ($\lambda > 300$ nm), Ar (1 atm), temperature (298 K), time (6 h).

^b Average diameter for metal nanoparticles determined by TEM observations. ^c Catalysts were reused after simple washing with ethanol.

^d Photoreaction was performed without benzonitrile.

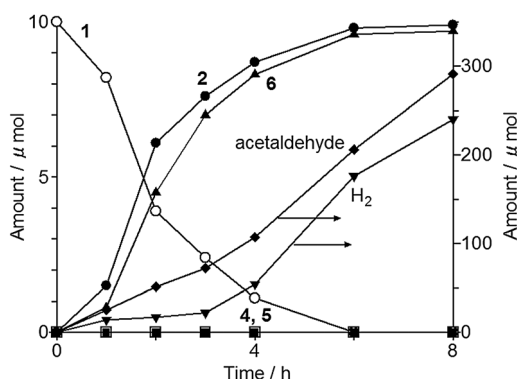
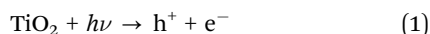


Fig. 4 Time-dependent change in the amounts of benzonitrile (1) and the products obtained during photoreaction of benzonitrile with the Pd₂-TiO₂ catalyst. Reaction conditions are identical to those in Table 2.

change in the amounts of benzonitrile and products during photoreaction with the Pd₂-TiO₂ catalyst. Photoirradiation leads to a decrease in the amount of benzonitrile, along with the formation of toluene and triethylamine. The profile for the toluene formation is very similar to that for the triethylamine formation. These data clearly suggest that the nitrogen atom of benzonitrile is removed as triethylamine.

3.3 Mechanism for photocatalytic hydrodenitrogenation

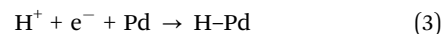
Photocatalytic hydrodenitrogenation of benzonitrile is initiated by photoexcitation of TiO₂. This produces the positive hole (h⁺) and electron (e⁻) pairs, as follows.



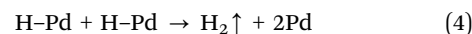
The h⁺ oxidizes ethanol and produces acetaldehyde and protons (H⁺) on the TiO₂ surface.^{18,20}



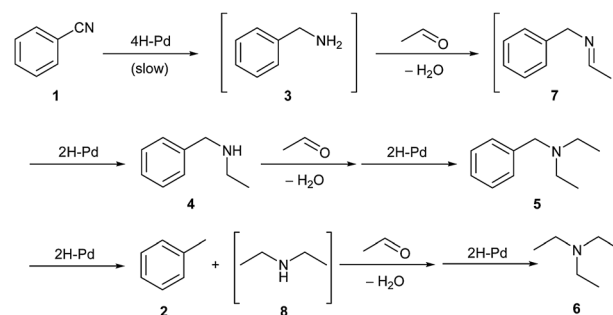
The photoformed conduction band e⁻ is transferred to the Pd particles. This reduces H⁺ and produces a hydrogen atom on the particles (H-Pd species).



The parts of the hydrogen atoms on the Pd particles are removed by the coalescence as a H₂ gas.



The stoichiometrical conversion of benzonitrile to toluene and triethylamine (Fig. 4) indicates that three aldehyde molecules formed by the photocatalytic oxidation of ethanol (eqn (2)) are involved in the hydrodenitrogenation of one benzonitrile molecule. The reaction mechanism can therefore be summarized in Scheme 1, which involves twelve H-Pd species. The substrate benzonitrile (1) undergoes hydrogenation by the H-Pd species and produces benzylamine (3) intermediately. This is transformed to an imine intermediate (7) by condensation with acetaldehyde, and then converted to *N*-ethylbenzylamine (4) *via* hydrogenation by the H-Pd species. Condensation of 4 with acetaldehyde and subsequent hydrogenation by H-Pd species afford *N,N*-diethylbenzylamine (5).²¹ Hydrogenolysis of 5 by the H-Pd species produces toluene (2) and diethylamine (8). Condensation of 8 with acetaldehyde and subsequent hydrogenation produce triethylamine (6). During the photoreaction (Fig. 4), trace amounts of 4 and 5 (<0.1 μ mol) were detected by GC analysis. In addition, as summarized in Table 3, photocatalytic



Scheme 1 Proposed mechanism for photocatalytic hydrodenitrogenation of benzonitrile with Pd-TiO₂ catalysts in the presence of acetaldehyde.

Table 3 Results of photocatalytic reaction of various substrates with the Pd₂-TiO₂ catalyst^a

Substrate	Conversion/%	Yield/%	
		Toluene (2)	Triethylamine (6)
3	>99	99	97
4	>99	99	98
5	>99	>99	97

reactions of compounds 3, 4, or 5 as the starting material with the Pd₂-TiO₂ catalyst also produce toluene and triethylamine with almost quantitative yields. These findings clearly support the proposed denitrogenation mechanism involving the condensation with aldehyde and the hydrogenation by the H-Pd species (Scheme 1). As shown in Fig. 4, the mass balance of benzonitrile (1) and toluene (2) is almost 100% during the reaction. This suggests that the hydrogenation of 1 to 3 is the rate-determining step for this reaction sequence. Table 2 (run 9) shows the result of photocatalytic reaction performed in the absence of benzonitrile. The photoreaction produces 248 μmol H₂, which is larger than that obtained with benzonitrile (176 μmol, run 4). This indicates that hydrodenitrogenation and H₂ evolution (eqn (4)) take place competitively.

3.4 Hydrodenitrogenation of substituted benzonitrile

The Pd-TiO₂ catalyst was employed for hydrodenitrogenation of aromatic cyanides with several substituents. The results are summarized in Table 4. As shown in run 2, terephthalonitrile is successfully transformed to *p*-xylene with 98% yield *via* the hydrodenitrogenation of two -CN groups. Reaction of 1-naphthonitrile (run 3) produces 1-methylnaphthalene with 93% yield. Reactions of benzonitrile with methyl, methoxy, or hydroxyl substituents (runs 4–6) produce the corresponding toluene derivatives while maintaining these substituents. In contrast, halogens or carbonyl substituents also undergo reaction. As shown in run 7, the reaction of *p*-chlorobenzonitrile produces toluene because the halogen groups are removed *via* the reaction with H-Pd species.¹⁵ In addition, the carbonyl substituent is converted to the hydroxyl group (run 8) due to the reduction by the H-Pd species. These results suggest that the Pd-TiO₂ catalyst promotes hydrodenitrogenation of the -CN group even in the presence of substituents, although some substituents are also transformed during the reaction.

The Hammett plot analysis was carried out to clarify the effect of substituents on the reaction kinetics. Photocatalytic reactions of the above *p*-substituted benzonitriles were carried out with Pd₂-TiO₂ for 1 h, and the first-order rate constants for the decrease in substrate concentration, k (mM h⁻¹), were determined. Fig. 5 shows the relationship between log k and the substituent constant, σ .²² A linear correlation is observed, and the slope of the plot (ρ) is determined to be +0.795. The positive ρ value indicates that stabilization of the negative charge in the transition state efficiently promotes the reaction;

Table 4 Results of photocatalytic hydrodenitrogenation of various aromatic cyanides with the Pd₂-TiO₂ catalyst^a

Run	Substrate	Time/h	Substrate conversion/%	Product	Yield/%
1		12	>99		98
2		48	>99		98
3		24	>99		93
4		12	>99		93
5		12	>99		>99
6		48	>99		99
7		12	>99		93
8		12	>99		99

^a Reaction conditions: Pd₂-TiO₂ (10 mg), substrate (10 μmol), ethanol (5 mL), Xe lamp ($\lambda > 300$ nm), Ar (1 atm), temperature (298 K).

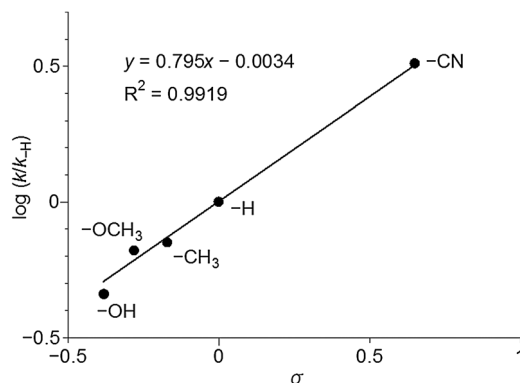


Fig. 5 Hammett plot for the photocatalytic reaction of *p*-substituted benzonitriles with Pd₂-TiO₂. The k denotes the first-order rate constant for the decrease in substrate concentration (mM h⁻¹) determined by 1 h photoreaction. The reaction conditions are identical to those in Table 4.

in other words, the reaction proceeds *via* a nucleophilic attack by a nucleophile.^{23–25} As proposed in Scheme 1, the reaction of benzonitrile (1) would occur *via* the hydrogenation of the -CN group (formation of benzylamine 3), *via* the nucleophilic attack by the H-Pd species. The Hammett plot results clearly support this mechanism.

3.5 Effect of Pd amount on the catalytic activity

As shown in Table 2, the denitrogenation activity depends on the amount of Pd loaded, and the Pd₂-TiO₂ catalyst shows the highest activity. The H-Pd species are formed on the surface Pd

atoms and, hence, the number of surface Pd atoms would strongly affect the denitrogenation activity. As shown in Fig. 2, the high-resolution TEM images of catalysts revealed that the shape of Pd particles is a part of a cuboctahedron surrounded by the (111) and (100) facets. The Pd particles on TiO₂ can therefore simply be modeled as an fcc cuboctahedron.²⁶ This structure is generally used as a model for cubic fcc metal nanoparticles. The numbers of surface metal atoms calculated based on this model are often employed for the determination of the active site in several catalytic systems such as hydrogenation of allyl alcohols with H₂ on Pd particles,²⁷ steam reforming of methane on Pt particles,²⁸ and oxidation of cinnamyl alcohols on Au particles.²⁹ The fcc cuboctahedron model therefore allows rough determination of the number of surface Pd atoms on the nanoparticles. Considering the full shell close packing cuboctahedron for Pd particles where one Pd atom is surrounded by twelve others, the number of total Pd atoms per Pd particle (N_{total}^*) is expressed by eqn (5) using the number of shells (m). N_{total}^* is rewritten with the average diameter of Pd particles (d_{Pd} /nm) and the atomic diameter of Pd (0.274 nm).³⁰ The number of surface Pd atoms per Pd particle (N_{surface}^*) is expressed by eqn (6).

$$N_{\text{total}}^*(-) = \frac{10m^3 - 15m^2 + 11m - 3}{3} = \left(\frac{d_{\text{Pd}}}{1.105 \times 0.274} \right)^3 \quad (5)$$

$$N_{\text{surface}}^*(-) = 10m^2 - 20m + 12 \quad (6)$$

The number of Pd particles per gram of the catalyst (n_{particle}) is expressed by eqn (7), using the percent amount of Pd loaded on the catalyst [x (wt%) = Pd/(Pd + TiO₂) × 100], molecular weight of Pd [M_{W} (= 106.42 g mol⁻¹)], and N_{total}^* . The number of surface Pd atoms per gram of the catalyst (N_{surface}) is therefore expressed by eqn (8).

$$n_{\text{particle}}(\text{mol g}^{-1}) = \frac{x}{100 \times M_{\text{W}} \times N_{\text{total}}^*} \quad (7)$$

$$N_{\text{surface}}(\text{mol g}^{-1}) = N_{\text{surface}}^* \times n_{\text{particle}} \quad (8)$$

The N_{surface} values for respective Pd_{*x*}-TiO₂ catalysts can therefore be calculated using their d_{Pd} values determined by the TEM observations (Fig. 1). As shown by the open symbols in Fig. 6, the N_{surface} values increase with an increase in the amount of Pd loaded; the values are 19.8 μmol g⁻¹ (Pd_{0.5}-TiO₂), 27.8 (Pd₁-TiO₂), 45.5 (Pd₂-TiO₂), and 73.1 (Pd₄-TiO₂), respectively. To clarify the hydrodenitrogenation activity per surface Pd atom, the turnover number for the reaction per surface Pd atom on respective catalyst (TON_{surface}) was determined based on eqn (9), using the amount of toluene formed (mol) during the photocatalytic reaction of benzonitrile for 6 h in the presence of 10 mg catalyst (Table 2).

$$\text{TON}_{\text{surface}}(-) = \frac{[\text{toluene formed}]}{N_{\text{surface}} \times 10 \times 10^{-3}} \quad (9)$$

As shown by the black symbols in Fig. 6, the TON_{surface} values for Pd_{0.5}-TiO₂, Pd₁-TiO₂, and Pd₂-TiO₂ are almost the same. This suggests that these catalysts produce the surface H-Pd

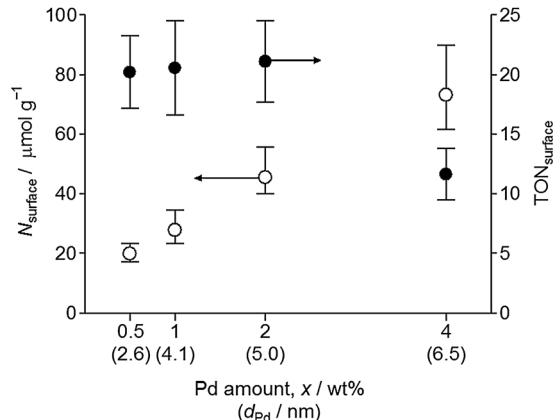


Fig. 6 (Open symbol) The number of surface Pd atoms per gram of Pd_{*x*}-TiO₂ catalysts (N_{surface}), and (closed symbol) the turnover number for toluene formation per surface Pd atom on respective catalysts during photocatalytic reaction of benzonitrile (TON_{surface}). Reaction conditions for benzonitrile were identical to those in Table 2.

species with similar efficiency. The higher activity of Pd₂-TiO₂ than Pd_{0.5}-TiO₂ and Pd₁-TiO₂ (Table 2) is therefore because a larger number of surface H-Pd species are produced due to the larger number of surface Pd atoms (N_{surface}).

In contrast, the TON_{surface} value of Pd₄-TiO₂ is much lower than that of lower Pd loading catalysts (Fig. 6), suggesting that the efficiency for H-Pd formation on the catalyst is lower. This is because the photocatalytic oxidation and reduction efficiency is decreased by the amount of Pd loaded. As shown in runs 2–5 (Table 2), the amounts of acetaldehyde and H₂ produced on Pd₄-TiO₂ are much lower than those on lower Pd loading catalysts. It is well known that, as shown in Fig. 7, the metal-semiconductor heterojunction creates a Schottky barrier (ϕ_{B}), and the ϕ_{B} height increases with an increase in the amount of metal loaded.³¹ The increased ϕ_{B} height by the increased Pd loadings therefore suppresses smooth transfer of the conduction band e⁻ to the Pd particles. This may result in inefficient charge separation between h⁺ and e⁻ and exhibit decreased photocatalytic activity. As a consequence, the H-Pd formation is suppressed, thus resulting in decreased denitrogenation

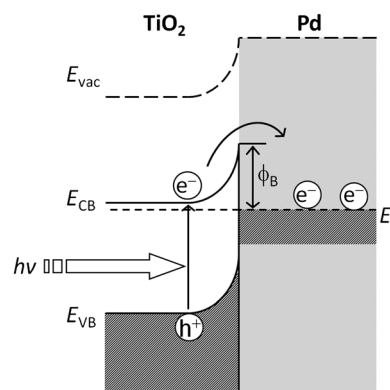


Fig. 7 Schematic representation of the Schottky barrier created at the Pd-TiO₂ heterojunction.

activity. These findings indicate that the Pd₂-TiO₂ catalyst, with relatively low ϕ_B height and a large number of surface Pd atoms, exhibits the highest activity for photocatalytic hydrodenitrogenation of aromatic cyanides.

4. Conclusion

TiO₂ loaded with Pd particles (Pd-TiO₂) was used as a catalyst for photocatalytic hydrodenitrogenation of aromatic cyanides in ethanol as a hydrogen source. These catalysts, when irradiated by UV light at room temperature, promote denitrogenation and produce the corresponding toluene derivatives and triethylamine with very high selectivity. Photoexcited Pd-TiO₂ produces acetaldehyde and the active H-Pd species. Consecutive reactions involving hydrogenation by H-Pd species and condensation with aldehyde facilitate efficient hydrodenitrogenation. The amount of Pd loaded and the size of Pd particles strongly affect the denitrogenation activity. The Pd-TiO₂ catalyst with a relatively low Schottky barrier height at the Pd-TiO₂ heterojunction and a large number of surface Pd atoms is necessary for efficient denitrogenation.

Acknowledgements

This work was supported by the Grant-in-Aid for Scientific Research (no. 23360349) from the Ministry of Education, Culture, Sports, Science and Technology, Japan (MEXT).

Notes and references

- 1 T. Li, J. Liu, R. Bai, D.-G. Ohandja and F.-S. Wong, *Water Res.*, 2007, **41**, 3465–3473.
- 2 G. Marci, A. D. Paola, E. García-López and L. Palmisano, *Catal. Today*, 2007, **129**, 16–21.
- 3 L. Martinková, B. Uhnáková, M. Pátek, J. Nešvera and V. Křen, *Environ. Int.*, 2009, **35**, 162–177.
- 4 P. Calza, E. Pelizzetti and C. Minero, *J. Appl. Electrochem.*, 2005, **35**, 665–673.
- 5 K. Okamoto, Y. Yamamoto, H. Tanaka, M. Tanaka and A. Itaya, *Bull. Chem. Soc. Jpn.*, 1985, **58**, 2015–2022.
- 6 H. Ohde, C. M. Wai, H. Kim, J. Kim and M. Ohde, *J. Am. Chem. Soc.*, 2002, **124**, 4540–4541.
- 7 J. Silvestre-Albero, G. Rupprechter and H.-J. Freund, *Chem. Commun.*, 2006, 80–82.
- 8 W. Ludwig, A. Savara, S. Schauermaun and H.-J. Freund, *ChemPhysChem*, 2010, **11**, 2319–2322.
- 9 W. Ludwig, A. Savara, K.-H. Dostert and S. Schauermaun, *J. Catal.*, 2011, **284**, 148–156.
- 10 D. K. Yi, S. S. Lee and J. Y. Ying, *Chem. Mater.*, 2006, **18**, 2459–2461.
- 11 X. Huang, Y. Wang, X. Liao and B. Shi, *Chem. Commun.*, 2009, 4687–4689.
- 12 H. Wu, L. Zhuo, Q. He, X. Liao and B. Shi, *Appl. Catal., A*, 2009, **366**, 44–56.
- 13 J. J. W. Bakker, A. G. van der Neut, M. T. Kreutzer, J. A. Moulijn and F. Kapteijn, *J. Catal.*, 2010, **274**, 176–191.
- 14 T. Sreethawong and S. Yoshikawa, *Catal. Commun.*, 2005, **6**, 661–668.
- 15 Y. Shiraishi, Y. Takeda, Y. Sugano, S. Ichikawa, S. Tanaka and T. Hirai, *Chem. Commun.*, 2011, **47**, 7863–7865.
- 16 Y. Shiraishi, D. Tsukamoto, Y. Sugano, A. Shiro, S. Ichikawa, S. Tanaka and T. Hirai, *ACS Catal.*, 2012, **2**, 1984–1992.
- 17 D. Tsukamoto, Y. Shiraishi, Y. Sugano, S. Ichikawa, S. Tanaka and T. Hirai, *J. Am. Chem. Soc.*, 2012, **134**, 6309–6315.
- 18 Y. Shiraishi, Y. Sugano, S. Tanaka and T. Hirai, *Angew. Chem., Int. Ed.*, 2010, **49**, 1656–1660.
- 19 D. Tsukamoto, A. Shiro, Y. Sugano, Y. Shiraishi, S. Ichikawa, S. Tanaka and T. Hirai, *ACS Catal.*, 2012, **2**, 599–603.
- 20 Y. Shiraishi and T. Hirai, *J. Photochem. Photobiol., C*, 2008, **9**, 157–170.
- 21 Y. Matsushita, N. Ohba, T. Suzuki and T. Ichimura, *Catal. Today*, 2008, **132**, 153–158.
- 22 K. A. Connors, *Chemical Kinetics, The Study of Reaction Rates in Solution*, VCH, New York, 1990.
- 23 X. Yang, L. Zhao, T. Fox, Z.-X. Wang and H. Berke, *Angew. Chem., Int. Ed.*, 2010, **49**, 2058–2062.
- 24 R. L. Donkers, Y. Song and R. W. Murray, *Langmuir*, 2004, **20**, 4703–4707.
- 25 P. Lu and N. Toshima, *Bull. Chem. Soc. Jpn.*, 2000, **73**, 751–758.
- 26 R. E. J. Benfield, *J. Chem. Soc., Faraday Trans.*, 1992, **88**, 1107–1110.
- 27 O. M. Wilson, M. R. Knecht, J. C. Gareia-Martinez and R. M. Crooks, *J. Am. Chem. Soc.*, 2006, **128**, 4510–4511.
- 28 Y. Qu, A. M. Sutherland, J. Lien, G. D. Suarez and T. Guo, *J. Phys. Chem. Lett.*, 2010, **1**, 254–259.
- 29 A. Abad, A. Corma and H. García, *Chem.–Eur. J.*, 2008, **14**, 212–222.
- 30 L. Pauling, *J. Am. Chem. Soc.*, 1947, **69**, 542–553.
- 31 T. Uchihara, M. Matsumura, A. Yamamoto and H. Tsubomura, *J. Phys. Chem.*, 1989, **93**, 5870–6874.